International Journal of Mycobacteriology 3 (2014) 117–126

Available at www.sciencedirect.com

ScienceDirect

journal homepage: www.elsevier.com/locate/IJMYCO

Investigating structure–activity relationship and mechanism of action of antitubercular 1-(4-chlorophenyl)-4-(4-hydroxy-3-methoxy-5-nitrobenzylidene) pyrazolidine-3,5-dione [CD59]

Ganesh Samala, Shruti Singh Kakan, Radhika Nallangi, Parthiban Brindha Devi, Jonnalagadda Padma Sridevi, Shalini Saxena, Perumal Yogeeswari, Dharmarajan Sriram *

Department of Pharmacy, Birla Institute of Technology & Science – Pilani, Hyderabad Campus, Jawahar Nagar, Hyderabad 500 078, India

ARTICLE INFO

Article history:
Received 23 January 2014
Received in revised form
25 February 2014
Accepted 25 February 2014
Available online 25 March 2014

Keywords:
Mycobacterium tuberculosis
Pantothenate synthetase
Lysine amino transferase
Alanine dehydrogenase

ABSTRACT

Background and objectives: The objective of this study is to synthesize and evaluate 1-(4-chlorophenyl)-4-(4-hydroxy-3-methoxy-5-nitrobenzylidene) pyrazolidine-3,5-dione (**CD59**) analogues to establish structure–activity relationship and mechanism of action.
Methods: Thirty analogues of reported antitubercular **CD59** were prepared by two-step synthetic protocols and characterized. The compounds were evaluated for *in vitro* activities against *Mycobacterium tuberculosis* (MTB), cytotoxicity against RAW 264.7 cells. The molecules were also evaluated for three mycobacterial enzymes to study the mechanism of action.
Results: Among the compounds, 4-(2-bromobenzylidene)-1-(4-chlorophenyl)pyrazolidine-3,5-dione (**4k**) was found to be the most active compound *in vitro* with MICs of 4.13 μM against log-phase culture of MTB and also non-toxic up to 50 μM.
Conclusions: Amongst all, the compounds **4g**, **3i** and **3n** were most active against the enzymes MTB Pantothenate synthetase, lysine amino transferase and Alanine dehydrogenase, respectively. Further screening of these molecules was required in the *in vitro* dormant MTB models.

Introduction

Tuberculosis (TB) is an infection that mainly affects the lungs and is caused by the pathogen *Mycobacterium tuberculosis* (MTB). In 2010, the World Health Organization estimated 8.8 million new cases of TB worldwide [1]. Since the disease remains a global health crisis with an alarming rise of multi-drug resistant and extensively drug resistant [2] bacterial strains, the need for new antitubercular therapeutics is very urgent. Target-based approaches are widely used in drug discovery; questions have been raised about the efficiency of this approach given the very high attrition rates that these projects have historically shown in the anti-infective field [3]. This situation becomes particularly alarming when consider-

* Corresponding author. Tel.: +91 40 66303506.
E-mail address: dsriram@hyderabad.bits-pilani.ac.in (D. Sriram).
http://dx.doi.org/10.1016/j.ijmyco.2014.02.006

ing the very limited number of validated targets for TB drug discovery. Furthermore, the state of affairs is a symptom of wider inconsistencies between results obtained with animal models of infection and their translation to clinical therapeutic value in humans. Compounds identified in whole-cell screens fulfil a double function: (a) they provide lead structures for further optimization within the drug development progression sequence, and (b) they can be exploited as tools to identify new targets. Notably, cell-based hits already fulfil some important criteria, including permeability issues and, given the progression criteria in the high-throughput screen, higher activity against mycobacteria than mammalian cells. Thus, they provide suitable chemical and biological starting points. Recently, William R. Jacobs, Jr. et al. [4] used a subset of a chemical library composed of 300 compounds inhibiting *Plasmodium falciparum* enoyl reductase, and tested it against MTB. Among them, one of the molecule **CD59** (1-(4-chlorophenyl)-4-(4-hydroxy-3-methoxy-5-nitrobenzylidene) pyrazolidine-3,5-dione) showed good activity against MTB with minimum inhibitory concentration (MIC) of 1.5 μM (Fig. 1). **CD59** was taken as the starting point to design more analogues by keeping pyrazolidine-3,5-dione nucleus intact and modify 1st and 4th positions with various aryl and heteroaryl moiety to investigate the structure- activity relationship (SAR) of the lead compound.

Materials and methods

Chemistry

All the reagents obtained from commercial sources were used without further purification. All reactions were run under an inert atmosphere of nitrogen or argon. All the reactions were monitored by thin layer chromatography (TLC) on silica gel 40 F254 (Merck, Darmstadt, Germany) coated on aluminum plates. All ^{1}H NMR spectra were recorded on a Bruker AM-300 and 400 NMR spectrometer, Bruker BioSpin Corp., Germany. Chemical shifts are in parts per million (ppm). Temperatures are reported in degrees Celsius (°C) and are uncorrected. Compounds were analysed for C, H, N, and analytical results obtained were within ±0.4% of the calculated values for the formula shown. Molecular weights of the synthesized compounds were checked by (Shimadzu, LCMS-2020) ESI-MS method.

General procedure for the preparation of compound **2**

To the stirred solution of (sub) phenylhydrazine (1.00 equiv) in ethanol under N_2 atmosphere added malonyl chloride (1.05 equiv) and the reaction mixture was stirred under reflux conditions for 3 h. The reaction mixture was concentrated to get a crude compound. The crude compound was purified by column chromatography (EtOAc/Hexanes as eluent) to get a pure compound (**2**).

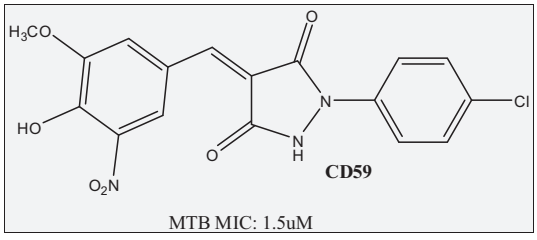

Fig. 1 – Reported antitubercular compound.

Preparation of 1-phenylpyrazolidine-3,5-dione

To the stirred solution of phenylhydrazine (3.0 g, 27.77 mmol) in ethanol under N_2 atmosphere was added malonyl chloride (2.81 mL, 29.16 mmol), and the reaction mixture was stirred under reflux conditions for 3 h. After completion of the reaction by checking TLC, the reaction mixture was concentrated to get a crude compound. The crude compound was directly purified by column chromatography (EtOAc/Hexanes as eluent) to get 1-phenylpyrazolidine-3,5-dione (3.60 g, 74%) as an off-white solid. ESI-MS showed 177 $[M+H]^+$ and was carried to the next step.

General procedure for the preparation of compound **3**

Compound **2** (1.0 equiv) and aldehyde (1.0 equiv) were taken in acetic acid and heated at 100 °C for 4 h. The solids formed in the reaction mixture were filtered and washed with water, cold EtOH and Hexanes to get compound **3** as an off-white solid.

*4-Benzylidene-1-phenylpyrazolidine-3,5-dione (***3a***)*

1-phenylpyrazolidine-3,5-dione (0.6 g, 3.41 mmol) and Benzaldehyde (0.34 mL, 3.41 mmol) were taken in acetic acid and heated at 100 °C for 4 h. The solids formed in the reaction mixture were filtered and washed with water, cold EtOH and hexanes to get (Z)-4-benzylidene-1-phenylpyrazolidine-3,5-dione (704 mg, 78%) as an off-white solid. MS(ESI) *m/z* 265 $[M+H]^+$. ^{1}H NMR (400 MHz, DMSO-d_6): δ 11.41 (bs, 1H), 8.49 (d, J = 7.2 Hz, 2H), 7.99–7.40 (m, 8H), 7.19 (t, J = 7.6 Hz, 1H). Anal calcd for $C_{16}H_{12}N_2O_2$: C, 72.72; H, 4.58; N, 10.60%. Found C, 72.81; H, 4.61; N, 10.71%.

*4-(4-Hydroxybenzylidene)-1-phenylpyrazolidine-3,5-dione (***3b***)*

MS(ESI) *m/z* 281 $[M+H]^+$. ^{1}H NMR (400 MHz, DMSO-d_6): δ 11.23 (s, 1H), 9.54 (s, 1H), 7.92–7.81 (m, 4H), 7.72 (s, 1H), 7.69(d, J = 7.2 Hz, 2H), 7.63–7.56 (m, 3H). Anal calcd for $C_{16}H_{12}N_2O_3$: C, 68.56; H, 4.32; N, 9.99%. Found C, 68.61; H, 4.41; N, 10.03%.

*4-(4-Methoxybenzylidene)-1-phenylpyrazolidine-3,5-dione (***3c***)*

MS(ESI) *m/z* 295 $[M+H]^+$. ^{1}H NMR (400 MHz, DMSO-d_6): δ 11.10 (s, 1H), 8.08 (d, J = 7.2 Hz, 2H), 7.90 (d, J = 7.6 Hz, 2H), 7.81 (s, 1H), 7.77–7.63 (m, 3H), 7.54 (d, J = 8.0 Hz, 2H), 4.03 (s, 3H). Anal calcd for $C_{17}H_{14}N_2O_3$: C, 69.38; H, 4.79; N, 9.52%. Found C, 69.41; H, 4.91; N, 9.58%.

4-(4-(Benzyloxy)benzylidene)-1-phenylpyrazolidine-3,5-dione (3d)

MS(ESI) *m*/z 371 $[M+H]^+$. ^1H NMR (400 MHz, DMSO-d_6): δ 11.22 (s, 1H), 7.92 (d, J = 7.6 Hz, 2H), 7.81–7.77 (m, 6H), 7.63 (d, J = 7.6 Hz, 2H), 7.58–7.49 (m, 5H), 5.20 (s, 2H). Anal calcd for $C_{23}H_{18}N_2O_3$: C, 74.58; H, 4.90; N, 7.56%. Found C, 74.61; H, 4.99; N, 7.63%.

4-(2-(Benzyloxy)benzylidene)-1-phenylpyrazolidine-3,5-dione (3e)

MS(ESI) *m*/z 371 $[M+H]^+$. ^1H NMR (400 MHz, DMSO-d_6): δ 11.28 (s, 1H), 7.92–7.81 (m, 4H), 7.77 (s, 1H), 7.72–7.58 (m, 6H), 7.54–7.45 (m, 4H), 5.10 (s, 2H). Anal calcd for $C_{23}H_{18}N_2O_3$: C, 74.58; H, 4.90; N, 7.56%. Found C, 74.63; H, 4.93; N, 7.68%.

4-(4-Methylbenzylidene)-1-phenylpyrazolidine-3,5-dione (3f)

MS(ESI) *m*/z 279 $[M+H]^+$. ^1H NMR (400 MHz, DMSO-d_6): δ 10.91 (s, 1H), 7.99 (d, J = 7.2 Hz, 2H), 7.81 (d, J = 7.2 Hz, 2H), 7.78 (s, 1H), 7.72–7.58 (m, 3H), 7.48 (d, J = 8.0 Hz, 2H), 2.63 (s, 3H). Anal calcd for $C_{17}H_{14}N_2O_2$: C, 73.37; H, 5.07; N, 10.07%. Found C, 73.41; H, 5.11; N, 10.15%.

1-Phenyl-4-(3,4,5-trimethoxybenzylidene)pyrazolidine-3,5-dione (3g)

MS(ESI) *m*/z 355 $[M+H]^+$. ^1H NMR (400 MHz, DMSO-d_6): δ 11.01 (s, 1H), 7.92 (d, J = 7.6 Hz, 2H), 7.81 (t, J = 6.8 Hz, 2H), 7.63 (t, J = 6.8 Hz, 1H), 7.54 (s, 1H), 7.36 (s, 2H), 3.94 (s, 9H). Anal calcd for $C_{19}H_{18}N_2O_5$: C, 64.40; H, 5.12; N, 7.91%. Found C, 64.47; H, 5.21; N, 7.99%.

4-(4-Fluorobenzylidene)-1-phenylpyrazolidine-3,5-dione (3h)

MS(ESI) *m*/z showed 283 $[M+H]^+$. ^1H NMR (400 MHz, DMSO-d_6): δ 11.61 (s, 1H), 8.10 (s, 1H), 7.81(d, J = 7.2 Hz, 2H), 7.72–7.54 (m, 5H), 7.49 (d, J = 7.6 Hz, 2H). Anal calcd for $C_{16}H_{11}FN_2O_2$: C, 68.08; H, 3.93; N, 9.92%. Found C, 68.11; H, 3.99; N, 9.97%.

4-(2-Chlorobenzylidene)-1-phenylpyrazolidine-3,5-dione (3i)

MS(ESI) *m*/z 299 $[M+H]^+$. ^1H NMR (400 MHz, DMSO-d_6): δ 11.31 (s, 1H), 7.99 (s, 1H), 7.81 (d, J = 7.6 Hz, 1H), 7.78–7.60 (m, 7H), 7.49 (t, 1H). Anal calcd for $C_{16}H_{11}ClN_2O_2$: C, 64.33; H, 3.71; N, 9.38%. Found C, 64.36; H, 3.76; N, 9.43%.

4-(4-Chlorobenzylidene)-1-phenylpyrazolidine-3,5-dione (3j)

MS(ESI) *m*/z 299 $[M+H]^+$. ^1H NMR (400 MHz, DMSO-d_6): δ 11.70 (s, 1H), 8.13 (s, 1H), 7.89 (d, J = 7.2 Hz, 2H), 7.76–7.49 (m, 7H). Anal calcd for $C_{16}H_{11}ClN_2O_2$: C, 64.33; H, 3.71; N, 9.38%. Found C, 64.36; H, 3.79; N, 9.43%.

4-(2-Bromobenzylidene)-1-phenylpyrazolidine-3,5-dione (3k)

MS(ESI) *m*/z 343 $[M+H]^+$. ^1H NMR (400 MHz, DMSO-d_6): δ 11.23 (s, 1H), 8.01 (s, 1H), 7.89 (d, J = 7.2 Hz, 1H), 7.81–7.63 (m, 7H), 7.54 (t, 1H). Anal calcd for $C_{16}H_{11}BrN_2O_2$: C, 56.00; H, 3.23; N, 8.16%. Found C, 56.10; H, 3.31; N, 8.21%.

4-(4-Bromobenzylidene)-1-phenylpyrazolidine-3,5-dione (3l)

MS(ESI) *m*/z 343 $[M+H]^+$. ^1H NMR (400 MHz, DMSO-d_6): δ 11.41 (s, 1H), 7.91(d, J = 7.2 Hz, 2H), 7.82 (d, J = 7.6 Hz, 2H), 7.78 (s, 1H), 7.72–7.63 (m, 3H), 7.49 (d, J = 7.2 Hz, 2H). Anal calcd for $C_{16}H_{11}BrN_2O_2$: C, 56.00; H, 3.23; N, 8.16%. Found C, 56.12; H, 3.33; N, 8.22%.

4-(3-Nitrobenzylidene)-1-phenylpyrazolidine-3,5-dione (3m)

MS(ESI) *m*/z 310 $[M+H]^+$. ^1H NMR (400 MHz, DMSO-d_6): δ 11.43 (s, 1H), 8.45 (s, 1H), 7.99 (d, J = 6.8 Hz, 1H), 7.92 (d, J = 7.2 Hz, 1H), 7.86 (s, 1H), 7.81 (d, J = 7.6 Hz, 2H), 7.72 (t, J = 6.8 Hz, 1H), 7.68–7.54 (m, 3H). Anal calcd for $C_{16}H_{11}N_3O_4$: C, 62.14; H, 3.58; N, 13.59%. Found C, 62.21; H, 3.60; N, 13.63%.

4-(Furan-2-ylmethylene)-1-phenylpyrazolidine-3,5-dione (3n)

MS(ESI) *m*/z 255 $[M+H]^+$. ^1H NMR (400 MHz, DMSO-d_6): δ 11.32 (s, 1H), 8.01 (d, J = 7.2 Hz, 1H), 7.92 (s, 1H), 7.81–7.74 (m, 3H), 7.63 (t, J = 7.2 Hz, 1H), 7.58–7.45 (m, 3H). Anal calcd for $C_{14}H_{10}N_2O_3$: C, 66.14; H, 3.96; N, 11.02%. Found C, 66.26; H, 4.03; N, 11.07%.

4-((5-Nitrofuran-2-yl)methylene)-1-phenylpyrazolidine-3,5-dione (3o)

MS(ESI) *m*/z 300 $[M+H]^+$. ^1H NMR (400 MHz, DMSO-d_6): δ 11.24 (s, 1H), 8.12 (d, J = 7.2 Hz, 1H), 7.89 (s, 1H), 7.78 (d, J = 7.2 Hz, 2H), 7.72 (t, J = 6.8 Hz, 1H), 7.62–7.49 (m, 3H). Anal calcd for $C_{14}H_9N_3O_5$: C, 56.19; H, 3.03; N, 14.04%. Found C, 56.26; H, 3.13; N, 14.08%.

4-Benzylidene-1-(4-chlorophenyl)pyrazolidine-3,5-dione (4a)

MS(ESI) *m*/z 299 $[M+H]^+$. ^1H NMR (400 MHz, DMSO-d_6): δ 11.22 (bs, 1H), 8.35 (d, J = 7.2 Hz, 2H), 8.10–7.81 (m, 4H), 7.72 (d, J = 6.8 Hz, 2H), 7.63–7.54 (m, 2H). Anal calcd for $C_{16}H_{11}ClN_2O_2$: C, 64.33; H, 3.71; N, 9.38%. Found C, 64.41; H, 3.76; N, 9.43%.

1-(4-Chlorophenyl)-4-(4-hydroxybenzylidene)pyrazolidine-3,5-dione (4b)

MS(ESI) *m*/z 315 $[M+H]^+$. ^1H NMR (400 MHz, DMSO-d_6): δ 11.10 (s, 1H), 9.63 (s, 1H), 8.01 (d, J = 7.6 Hz, 2H), 7.92–7.77 (m, 5H), 7.63 (d, J = 7.2 Hz, 2H). Anal calcd for $C_{16}H_{11}ClN_2O_3$: C, 61.06; H, 3.52; N, 8.90%. Found C, 61.12; H, 3.56; N, 8.98%.

1-(4-Chlorophenyl)-4-(4-methoxybenzylidene)pyrazolidine-3,5-dione (**4c**)

MS(ESI) *m*/z 329 $[M+H]^+$. ^1H NMR (400 MHz, DMSO-d_6): δ 11.32 (s, 1H), 7.92 (d, *J* = 7.6 Hz, 2H), 7.81 (d, *J* = 7.6 Hz, 2H), 7.76 (s, 1H), 7.65 (d, *J* = 7.6 Hz, 2H), 7.54 (d, *J* = 7.6 Hz, 2H), 4.12 (s, 3H). Anal calcd for $C_{17}H_{13}ClN_2O_3$: C, 62.11; H, 3.99; N, 8.52%. Found C, 62.21; H, 4.05; N, 8.64%.

4-(4-(Benzyloxy)benzylidene)-1-(4-chlorophenyl)pyrazolidine-3,5-dione (**4d**)

MS(ESI) *m*/z 405 $[M+H]^+$. ^1H NMR (400 MHz, DMSO-d_6): δ 11.45 (s, 1H), 8.02 (d, *J* = 7.2 Hz, 2H), 7.92 (d, *J* = 7.6 Hz, 2H), 7.87–7.72 (m, 4H), 7.63–7.58 (m, 4H), 7.45 (d, *J* = 8.0 Hz, 2H), 5.13 (s, 2H). Anal calcd for $C_{23}H_{17}ClN_2O_3$: C, 68.23; H, 4.23; N, 6.92%. Found C, 68.31; H, 4.29; N, 6.99%.

4-(2-(Benzyloxy)benzylidene)-1-(4-chlorophenyl)pyrazolidine-3,5-dione (**4e**)

MS(ESI) *m*/z 405 $[M+H]^+$. ^1H NMR (400 MHz, DMSO-d_6): δ 11.43 (s, 1H), 8.12–7.81 (m, 6H), 7.77–7.63 (m, 6H), 7.58–7.49 (m, 2H), 5.22 (s, 2H). Anal calcd for $C_{23}H_{17}ClN_2O_3$: C, 68.23; H, 4.23; N, 6.92%. Found C, 68.35; H, 4.26; N, 7.02%.

1-(4-Chlorophenyl)-4-(4-methylbenzylidene)pyrazolidine-3,5-dione (**4f**)

MS(ESI) *m*/z 313 $[M+H]^+$. ^1H NMR (400 MHz, DMSO-d_6): δ 11.31 (s, 1H), 7.92 (d, *J* = 7.2 Hz, 2H), 7.84 (d, *J* = 7.2 Hz, 2H), 7.78 (s, 1H), 7.71 (d, *J* = 7.6 Hz, 2H), 7.63 (d, *J* = 7.6 Hz, 2H), 2.58 (s, 3H). Anal calcd for $C_{17}H_{13}ClN_2O_2$: C, 65.29; H, 4.19; N, 8.96%. Found C, 65.41; H, 4.21; N, 9.07%.

1-(4-Chlorophenyl)-4-(3,4,5-trimethoxybenzylidene)pyrazolidine-3,5-dione (**4g**)

MS(ESI) *m*/z 389 $[M+H]^+$. ^1H NMR (400 MHz, DMSO-d_6): δ 11.24 (s, 1H), 7.99(d, *J* = 8.0 Hz, 2H), 7.83 (d, *J* = 7.6 Hz, 2H), 7.72 (s, 1H), 7.58 (s, 2H), 3.96 (s, 9H). Anal calcd for $C_{19}H_{17}ClN_2O_5$: C, 58.69; H, 4.41; N, 7.21%. Found C, 58.72; H, 4.49; N, 7.30%.

1-(4-Chlorophenyl)-4-(4-fluorobenzylidene)pyrazolidine-3,5-dione (**4h**)

MS(ESI) *m*/z 317 $[M+H]^+$. ^1H NMR (400 MHz, DMSO-d_6): δ 11.61 (s, 1H), 7.99 (d, *J* = 7.2 Hz, 2H), 7.81 (d, *J* = 7.2 Hz, 2H), 7.72 (d, *J* = 7.2 Hz, 2H), 7.65 (s, 1H), 7.49 (d, *J* = 7.2 Hz, 2H). Anal calcd for $C_{16}H_{10}ClFN_2O_2$: C, 60.68; H, 3.18; N, 8.85%. Found C, 60.72; H, 3.21; N, 8.91%.

4-(2-Chlorobenzylidene)-1-(4-chlorophenyl)pyrazolidine-3,5-dione (**4i**)

MS(ESI) *m*/z 333 $[M+H]^+$. ^1H NMR (400 MHz, DMSO-d_6): δ 10.31 (s, 1H), 7.89 (d, *J* = 7.2 Hz, 2H), 7.81 (s, 1H), 7.76–7.58 (m, 6H). Anal calcd for $C_{16}H_{10}Cl_2N_2O_2$: C, 57.68; H, 3.03; N, 8.41%. Found C, 57.70; H, 3.07; N, 8.54%.

4-(4-Chlorobenzylidene)-1-(4-chlorophenyl)pyrazolidine-3,5-dione (**4j**)

MS(ESI) *m*/z 333 $[M+H]^+$. ^1H NMR (400 MHz, DMSO-d_6): δ 11.70 (s, 1H), 8.01 (d, *J* = 7.2 Hz, 2H), 7.92 (d, *J* = 7.2 Hz, 2H), 7.72 (d, *J* = 7.2 Hz, 2H), 7.63 (s, 1H), 7.54 (d, *J* = 7.2 Hz, 2H). Anal calcd for $C_{16}H_{10}Cl_2N_2O_2$: C, 57.68; H, 3.03; N, 8.41%. Found C, 57.72; H, 3.12; N, 8.53%.

4-(2-Bromobenzylidene)-1-(4-chlorophenyl)pyrazolidine-3,5-dione (**4k**)

MS(ESI) *m*/z 377 $[M+H]^+$. ^1H NMR (400 MHz, DMSO-d_6): δ 11.22 (s, 1H), 7.81 (d, *J* = 7.2 Hz, 1H), 7.77 (s, 1H), 7.72–7.58 (m, 6H), 7.47 (d, *J* = 7.2 Hz, 1H). Anal calcd for $C_{16}H_{10}BrClN_2O_2$: C, 50.89; H, 2.67; N, 7.42%. Found C, 50.94; H, 2.74; N, 7.47%.

4-(4-Bromobenzylidene)-1-(4-chlorophenyl)pyrazolidine-3,5-dione (**4l**)

MS(ESI) *m*/z 377 $[M+H]^+$. ^1H NMR (400 MHz, DMSO-d_6): δ 11.43 (s, 1H), 8.04 (d, *J* = 7.2 Hz, 2H), 7.92 (d, *J* = 7.6 Hz, 2H), 7.69 (d, *J* = 8.0 Hz, 2H), 7.58 (s, 1H), 7.45 (d, *J* = 7.6 Hz, 2H). Anal calcd for $C_{16}H_{10}BrClN_2O_2$: C, 50.89; H, 2.67; N, 7.42%. Found C, 50.94; H, 2.72; N, 7.54%.

1-(4-Chlorophenyl)-4-(3-nitrobenzylidene)pyrazolidine-3,5-dione (**4m**)

MS(ESI) *m*/z 344 $[M+H]^+$. ^1H NMR (400 MHz, DMSO-d_6): δ 11.34 (s, 1H), 8.49 (s, 1H), 8.08–7.94 (m, 3H), 7.83 (d, *J* = 7.6 Hz, 2H), 7.76 (t, *J* = 6.8 Hz, 1H), 7.72 (d, *J* = 7.2 Hz, 2H). Anal calcd for $C_{16}H_{10}ClN_3O_4$: C, 55.91; H, 2.93; N, 12.23%. Found C, 55.97; H, 2.98; N, 12.34%.

1-(4-Chlorophenyl)-4-(furan-2-ylmethylene)pyrazolidine-3,5-dione (**4n**)

MS(ESI) *m*/z 289 $[M+H]^+$. ^1H NMR (400 MHz, DMSO-d_6): δ 11.43 (s, 1H), 8.12 (d, *J* = 7.2 Hz, 1H), 7.96 (d, *J* = 7.6 Hz, 1H), 7.89–7.79 (m, 3H), 7.76 (t, *J* = 6.8 Hz, 1H) 7.72 (d, *J* = 7.2 Hz, 2H). Anal calcd for $C_{14}H_9ClN_2O_3$: C, 58.25; H, 3.14; N, 9.70%. Found C, 58.31; H, 3.21; N, 9.81%.

1-(4-Chlorophenyl)-4-((5-nitrofuran-2-yl)methylene) pyrazolidine-3,5-dione (**4o**)

MS(ESI) *m*/z 334 $[M+H]^+$. ^1H NMR (400 MHz, DMSO-d_6): δ 11.49 (s, 1H), 8.28 (d, *J* = 7.2 Hz, 1H), 8.01 (d, *J* = 7.6 Hz, 1H), 7.89 (d, *J* = 8.0 Hz, 2H), 7.81 (s, 1H), 7.74 (d, *J* = 7.6 Hz, 2H). Anal calcd for $C_{14}H_8ClN_3O_5$: C, 50.39; H, 2.42; N, 12.59%. Found C, 50.45; H, 2.49; N, 12.71%.

Biological evaluation

In vitro MTB MABA assay

Briefly, the inoculum was prepared from fresh LJ medium re-suspended in 7H9 medium (7H9 broth, 0.1% casitone, 0.5%

glycerol, supplemented oleic acid, albumin, dextrose, and catalase [OADC]), adjusted to a McFarland tube No. 1, and diluted 1:20; 100 μl was used as inoculum. Each drug stock solution was thawed and diluted in 7H9-S at fourfold the final highest concentration tested. Serial twofold dilutions of each drug were prepared directly in a sterile 96-well microtiter plate using 100 μl 7H9-S. A growth control containing no antibiotic and a sterile control were also prepared on each plate. Sterile water was added to all perimeter wells to avoid evaporation during the incubation. The plate was covered, sealed in plastic bags and incubated at 37 °C in normal atmosphere. After 7 days of incubation, 30 μl of alamar blue solution was added to each well, and the plate was re-incubated overnight. A change in color from blue (oxidized state) to pink (reduced) indicated the growth of bacteria, and the MIC was defined as the lowest concentration of drug that prevented this change in color.

In vitro cytotoxicity screening

The safety profile of all the compounds were examined by evaluating their *in vitro* cytotoxicity against RAW 264.7 cell line at the concentration of 100 μM. After 72 h of exposure, viability was assessed on the basis of cellular conversion of MTT into a formazan product using the Promega Cell Titer 96 non-radioactive cell proliferation assay.

In vitro MTB Pantothenate synthetase screening

To each well of a 96-well plate, 60 μL of PS reagent mix was added, including NADH, pantoic acid, β-alanine, ATP, phosphoenolpyruvate, $MgCl_2$, myokinase, pyruvate kinase, and lactate dehydrogenase in buffer. Compounds were then added to plates in 1-μL volumes. The reaction was initiated with the addition of 39 μL of PS, diluted in buffer. The final concentrations in the reaction were 0.4 mM NADH, 5 mM pantoic acid, 10 mM $MgCl_2$, 5 mM β-alanine, 10 mM ATP, 1 mM potassium phosphoenolpyruvate, and 18 units/mL each of chicken muscle myokinase, rabbit muscle pyruvate kinase, and rabbit muscle lactate dehydrogenase diluted in 100 mM HEPES buffer (pH 7.8), 1% DMSO, and 5 μg/mL PS in a final volume of 100 μL. The test plate was immediately transferred to a microplate reader, and absorbance was measured at 340 nm every 12 s for 120 s. Each plate had 16 control wells in the 2 outside columns, of which 12 contained the complete reaction mixture with DMSO carrier control (full reaction) and 4 without the addition of PS (background).% Inhib calculated using the following formula: 100 * 1 – compound rate – background rate/full reaction rate – background rate.

In vitro MTB L-Alanine dehydrogenase (AlaDH) enzyme inhibition assay

To each well of a 96-well plate, reaction mixture consisted of 125 mM glycine/KOH (pH 10.2), 100 mM L-alanine, 1.25 mM NAD^+ and 6.026 pM of MTB-AlaDH in a final volume of 200 μl diluted in 125 mM glycine/KOH (pH 10.2). Compounds were then added to plates. The reaction was initiated with the addition of 10μL of ADH, diluted in buffer. Enzymatic activity was measured by the rate of the production of NADH that accompanies the conversion of alanine to pyruvate in the oxidative deamination. The reaction components, except MTB-AlaDH, were mixed in the well and the background reaction was measured; MTB-AlaDH was then added and the reaction kinetics was monitored. The same method was followed for testing the designed inhibitors with different concentrations. All measurements were performed at 340 nm with heat-controlled Perkin Elmer Victor V3 spectrophotometer.

In vitro MTB lysine amino transferase (LAT) enzyme inhibition assay

MTB LAT activity was determined by the detection of piperidine 6-carboxylate. Briefly, 15 mM enzyme solution was added to 1.0 ml 200 mM phosphate buffer pH 7.2 containing 1 mM L-lysine–HCl, 1 mM α-ketoglutarate and 15 mM PLP. The mixture was incubated at 310 K for 1 h. The reaction was terminated by the addition of 500 ml 10% trichloroacetic acid in ethanol. Piperidine 6-carboxylate was detected by measuring the color intensity of its adduct with o-aminobenzaldehyde spectroscopically at 465 nm.

Results

Biological evaluation

The compounds were screened for their *in vitro* antimycobacterial activity against *M. tuberculosis* H37Rv by microplate alamar blue assay method [5] for the determination of MIC in duplicate. The minimum inhibitory concentration (MIC) is defined as the minimum concentration of compound required to give complete inhibition of bacterial growth. MICs of the synthesized compounds along with the standard drugs for comparison are reported (Table 1).

Most of the tested compounds were not cytotoxic to RAW 264.7 cells and their percentage growth inhibitions were reported in Table 1. To explore the possible mechanism/target of these active antitubercular compounds, 20 compounds with MIC of $\leqslant$25 μM were selected and screened against MTB Pantothenate synthetase (PS), lysine amino transferase (LAT) and Alanine dehydrogenase enzymes (AlaDH). PS (EC 6.3.2.1), encoded by the *panC* gene, catalyzes the essential adenosine triphosphate (ATP)-dependent condensation of D-pantoate and β-alanine to form pantothenate in bacteria [6], and IC_{50} values were reported in Table 1.

Discussion

Chemistry

The target molecules were synthesized by two-step synthetic protocol (Fig. 2); in the first step, the (sub)phenylhydrazine was initially treated with malonic acid using methanol as a solvent under reflux conditions for 2 h. These reactions were also carried with malonyl chloride instead of malonic acid in ethanol as a solvent under reflux conditions for 3 h; more yields were observed when the reactions were carried using malonyl chloride. The commercially available 4-chlorophenylhydra-

Table 1 – Biological activities of synthesized compounds.

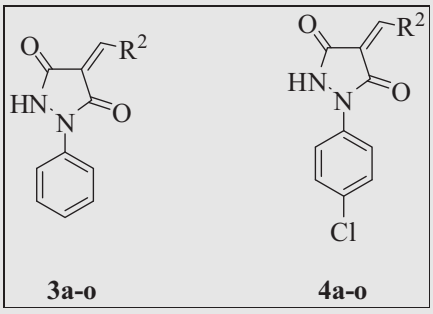

3a-o **4a-o**

Comp.	R^2	Yield (%)	MP (°C)	MTB MIC in μM	IC_{50} in μM PanC	IC_{50} in μM AlaDH	IC_{50} in μM LAT	Cytotoxicity at 50 μM[a]
3a	Phenyl	78	235–236	188.6	NT	NT	NT	NT
3b	4-Hydroxyphenyl	81	210–211	111.2	NT	NT	NT	NT
3c	4-Methoxyphenyl	65	198–199	84.74	NT	NT	NT	NT
3d	4-Benzyloxyphenyl	71	205–206	67.38	NT	NT	NT	NT
3e	2-Benzyloxyphenyl	69	213–214	134.77	NT	NT	NT	NT
3f	4-Methylphenyl	63	240–241	179.21	NT	NT	NT	NT
3g	3,4,5-Trimethoxyphenyl	79	260–261	140.84	NT	NT	NT	NT
3h	4-Fluorophenyl	54	191–192	5.53	5.47 ± 0.24	>50	50 ± 3.12	22.16
3i	2-Chlorophenyl	61	204–205	5.21	>50	>50	11.45 ± 0.16	18.12
3j	4-Chlorophenyl	72	241–242	5.21	>50	>50	29.92 ± 1.16	20.86
3k	2-Bromophenyl	65	187–188	4.54	>50	10.63 ± 0.16	>50	18.42
3l	4-Bromophenyl	70	178–179	18.22	>50	>50	21.40 ± 1.62	24.62
3m	3-Nitrophenyl	63	234–235	10.08	50 ± 1.32	>50	40.64 ± 3.24	30.16
3n	Furan-2-yl	57	245–246	24.5	>50	8.14 ± 0.09	>50	26.52
3o	5-Nitrofuran-2-yl	76	225–226	10.41	6.98 ± 0.12	>50	40.43 ± 2.12	28.32
4a	Phenyl	66	211–213	20.84	12.51 ± 0.08	22.39 ± 0.38	50 ± 2.68	16.12
4b	4-Hydroxyphenyl	52	214–215	15.87	4.18 ± 0.16	>50	>50	12.28
4c	4-Methoxyphenyl	76	231–232	37.99	NT	NT	NT	NT
4d	4-Benzyloxyphenyl	81	241–242	7.71	>50	8.97 ± 0.34	13.60 ± 0.92	14.56
4e	2-Benzyloxyphenyl	69	247–248	41.15	NT	NT	NT	NT
4f	4-Methylphenyl	74	229–231	53.31	NT	NT	NT	NT
4g	3,4,5-Trimethoxyphenyl	69	260–261	16.06	3.73 ± 0.11	15.84 ± 0.46	>50	11.86
4h	4-Fluorophenyl	54	219–220	7.88	6.14 ± 0.33	>50	>50	
4i	2-Chlorophenyl	64	222–223	4.68	12.98 ± 0.30	30.02 ± 0.64	19.94 ± 0.37	27.42
4j	4-Chlorophenyl	67	261–262	7.50	50 ± 2.08	50 ± 2.07	19.92 ± 0.12	23.14
4k	2-Bromophenyl	72	238–239	4.13	9.68 ± 0.26	19.47 ± 0.10	50 ± 2.41	26.12
4l	4-Bromophenyl	60	217–218	13.26	>50	50 ± 1.68	32.16 ± 1.60	18.12
4m	3-Nitrophenyl	63	223–224	18.16	>50	>50	30.42 ± 1.78	29.19
4n	Furan-2-yl	58	235–236	17.30	>50	12.46 ± 1.04	>50	16.18
4o	5-Nitrofuran-2-yl	62	246–247	7.48	10.16 ± 0.09	>50	>50	24.53
Isoniazid				0.72	>50	>50	>50	NT
Rifampicin				0.24	>50	>50	>50	NT
Ethambutol				7.64	>50	>50	>50	NT
Pyrazinamide				50.77	>50	>50	>50	NT
Ciprofloxacin				4.71	>50	>50	>50	NT

NT indicates not tested.

[a] % inhibition against RAW 264.7 cells.

zine is a hydrochloride salt; here the hydrochloride salt was first converted into a free amine by taking a compound in saturated $NaHCO_3$ solution, stirring for a few minutes, then extracting the free amine with dichloromethane; the evaporation of solvent produced the free amine. The obtained free amine was treated with malonyl chloride using ethanol under reflux conditions. The reaction mixture was concentrated and triturated with water to obtain solid compound, the solids were washed with water, cold ethanol, hexanes and dried *in vacuo* to get compound **2**. In the next step the active methylene group of compound **2** (1-substituted-pyrazolidine-3,5-dione) was condensed with various substituted aldehydes to produce target molecules (**3a–o**, **4a–o**). Here the compound **2** was refluxed and phenyl/heteroaryl aldehyde was substituted in acetic acid for 4 h. The formation of solids was observed in the reaction mixture; direct filtration of the reaction mixture and washing

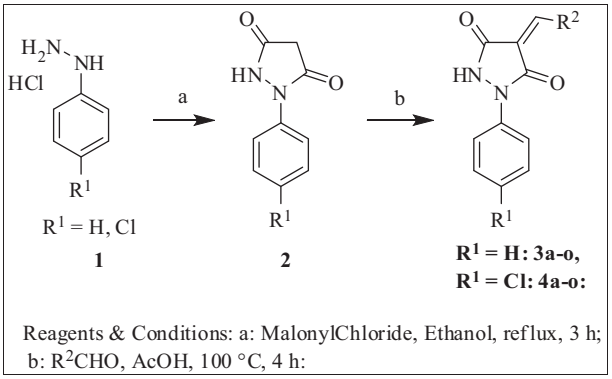

Fig. 2 – Synthetic protocol of the compounds.

of the residue with excess water removed the traces of acetic acid and then dried in a vacuum oven to get pure products with ease of purification and with good yields. The purity of the synthesized compounds was checked by TLC and elemental analyses, and the structures were identified by spectral data. In the nuclear magnetic resonance spectra (^{1}H NMR), the signals of the respective protons of the prepared pyrazolidinedione derivatives were verified on the basis of their chemical shifts, multiplicities, and coupling constants. The elemental analysis results were within ±0.4% of the theoretical values.

Antitubercular activity

The synthesized compounds showed MIC's ranging from 4.13–188.6 μM; and 11 compounds showed promising activity with MIC of less than 10 μM. When compared with original lead compound **CD59**, all the compounds were found to be less active. When compared with the standard first-line antitubercular drug ethambutol (MIC of 7.64 μM), 9 compounds were found to be more active, and when compared with pyrazinamide (MIC of 50.77 μM), 22 compounds were more active. All the molecules were found be less active than isoniazid (MIC of 0.72 μM) and rifampicin (MIC of 0.24 μM), but 3 compounds were more/equally active than/as DNA gyrase inhibitor ciprofloxacin (MIC of 4.71 μM). Among the compounds, 4-(2-bromobenzylidene)-1-(4-chlorophenyl)pyrazolidine-3,5-dione (**4k**) was found to be the most active compound *in vitro* with MICs of 4.13 μM.

SAR study

To study the SAR, the compounds were prepared with variations in 1st and 4th positions. In N-1 position, two types of modifications were tried: one with phenyl (**3a–o**) and the other with 4-chlorophenyl (**4a–o**) groups as of lead compound. In the C-4 position, molecules were prepared with a phenyl ring with both electrons donating and with drawing groups and also with a few heterocycles. The order of activity with respect to N-1 position found 4-chlorophenyl (**4a–o**) to be more potent than phenyl ring (**3a–o**). Phenyl ring at N-1 position and at C-3 position phenyl ring with electron donating groups (**3b–g**) were found to be more potent than phenyl ring with electron withdrawing groups (**3h–m**). Compound **3a**, without any substituent on either of the phenyl rings, displayed an MIC of 188.6 μM and serves as the standard for potency comparison. The activity of **3b** improved 1.6 times (111.2 μM) when a hydroxyl group was introduced at the 4th position of the phenyl ring at C-3. Replacement of hydroxyl group with methoxyl group (**3c**) further enhances the potency with MIC of 84.74 and it further increases with MIC of 67.38 μM by introducing bulky benzyloxy group at 4th position (**3d**). Whereas shifting benzyloxy group (**3e**) from 4th position to 2nd position reduces activity two times with MIC of 134.77 μM. Introduction of methyl group at 4th position (**3f**) does not change much difference in activity when compared with compound **3a**. Similarly, the introduction of three methoxyl groups (**3g**) also does not show promising activity (140.84 μM). The introduction of electron withdrawing group at 2nd, 3rd, and 4th position (**3h–m**) generally enhances potency ten or more times with MICs range from 4.54–18.22 μM. The introduction of the furan ring (**3n**) improved 7.6 times (24.5 μM) more than the compound **3a**, and the further introduction of the nitro group at the 5th position of the furan ring (**3o**) further enhances the activity (10.41 μM). In the case of a second set of compounds (**4a–o**) with 4-chloro phenyl ring at N-1 position, the introduction of the phenyl ring at the C-3 position (**4a**) makes it 9 times more potent than compound **3a**. The intro-

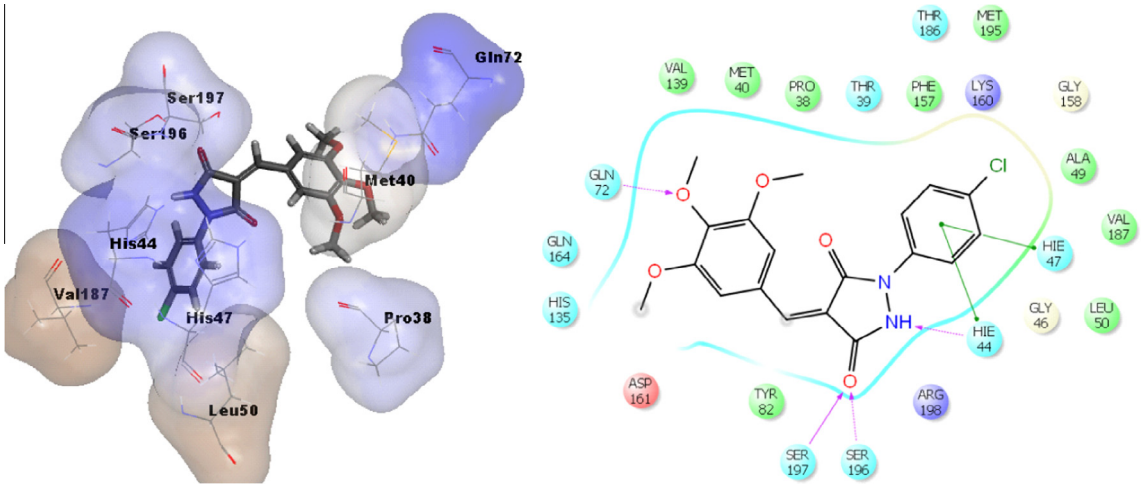

Fig. 3 – Binding pattern and protein ligand contacts of *PanC* with the most active compound 4g.

duction of the electron donating groups like hydroxyl, methoxy and methyl does not alter activity much except the 4-benzyloxy group (**4d**) which was three times more potent than compound **4a**. The compound with the electron withdrawing substituents (**4h–m**) was equal or less active than its counterpart with the first set (**3h–m**).

Cytotoxicity

Compounds which showed MIC of less than 25 μM were further examined for cytotoxicity (CC_{50}) in a RAW 264.7 cell line (mouse leukemic monocyte macrophage) at single concentration of 50 μM. After 72 h of exposure, viability was assessed on the basis of cellular conversion of MTT into a formazan product using the Promega Cell Titer 96 non-radioactive cell proliferation assay. The most active anti-TB compound **4k** has shown toxicity of 26.12% at 50 μM with selectivity index of >12.5 for MTB.

Enzyme inhibition and docking studies

Pantothenate is a key precursor of coenzyme A and acyl carrier protein, essential for many intracellular processes including fatty acid metabolism, cell signalling, and synthesis of polyketides and non-ribosomal peptides. Both microorganisms and plants must synthesize pantothenate, while mammals must obtain it from their diet, and its biosynthetic pathway is not present. A *PanC* gene knockout (KO) of PS in MTB results in a highly attenuated phenotype in immunocompromised SCID mice and in immunocompetent BALB/c mice [7], whereas the Δ*lysA* Δ*panCD* KO mutant exhibits substantially reduced replication and persistence [8]. The compounds were assayed for MTB PS inhibition study, that couples the AMP produced in the condensation of β-alanine and pantoate with the reduction of NADH to NAD^+ through myokinase, pyruvate kinase and lactate dehydrogenase [6]. The IC_{50} of the screened compounds were reported in Table 1, ten compounds inhibited MTB PS with IC_{50} of ⩽50 μM. Five compounds (**3h**, **3o**, **4b**, **4g** and **4k**) inhibited with IC_{50} of <10 μM, and compound 1-(4-chlorophenyl)-4-(3,4,5-trimethoxybenzylidene)pyrazolidine-3,5-dione (**4g**) emerged as more potent with IC_{50} of 3.73 ± 0.11 μM. Compound 4-(4-fluorobenzylidene)-1-phenylpyrazolidine-3,5-dione (**3h**) showed good correlation with MIC and IC_{50} of 5.53 and 5.47 ± 0.24 μM, respectively. The crystal structure of the protein *MTB PS* in complex with inhibitor 2-(2-(benzofuran-2ylsulfonylcarbamoyl)-5-methoxy-1H-indol-1-yl) acetic acid (PDB code: 3IVX) was retrieved from the protein data bank (PDB) and was used for docking [9]. Analysis of the crystal structure of 3IVX revealed two key hydrogen-bonding interactions, with the carboxyl group to Met40 and His47 each. Also, it was making hydrogen bonding interaction with Val187, Ser196, Ser197 and His44. The protein crystal structure has two hydrophobic pockets; one consists of Met40, Leu50, Phe157, Thr39 and Pro38, and the other consists of Lys160, His44 and Gly46. First the 2-(2-(benzofuran-2-ylsulfonylcarbamoyl)-5-methoxy-1H-indol-1-yl) acetic acid is used to re-dock the active site cavity, and it was showing a docking score of −9.03 and exhibiting same hydrogen bonding interactions as shown in the crystal structure of the protein. With the aim of getting insights into the structural basis for the present MTB PS activity, the most active compound **4g** in the series was docked into the active site of PanC enzyme. The most active compound **4g** exhibited the IC_{50} 3.73 ± 0.11 μM, and it shows a good docking score of −7.72 kcal/mol. The active compound **4g** showed four hydrogen bonding interactions with the relevant amino acid residues, such as HIE44, Ser197, Ser196 and Gln72. As shown in Fig. 3, 4-chlorophenyl is occupying the one hydrophobic pocket. The compound also showed π-π stacking interaction with HIE47 and HIE44 amino acid residues. Comparison of the enzyme inhibitory effectiveness of the compound **4g** with glide score suggests that the compound **4g** adopts almost the same conformation as reference compounds; also, out of five important amino acid residues (HIE47, Met40, HIE44, Ser196 and Val187), it made an interaction with three amino acid res-

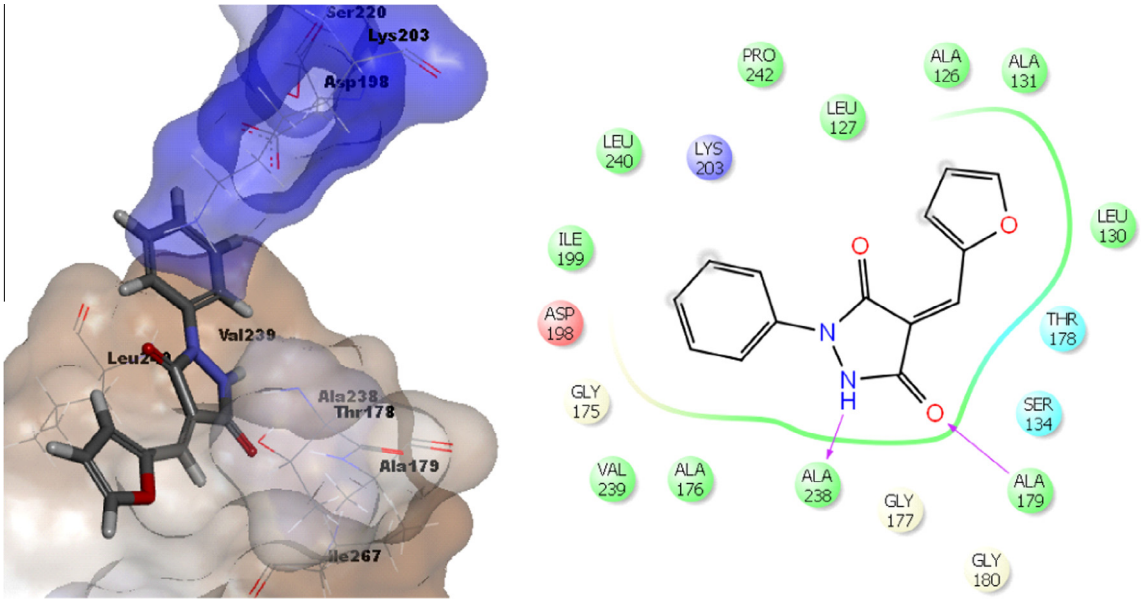

Fig. 4 – Binding pattern and protein ligand contacts of MTB AlaDH with the most active compound 3n.

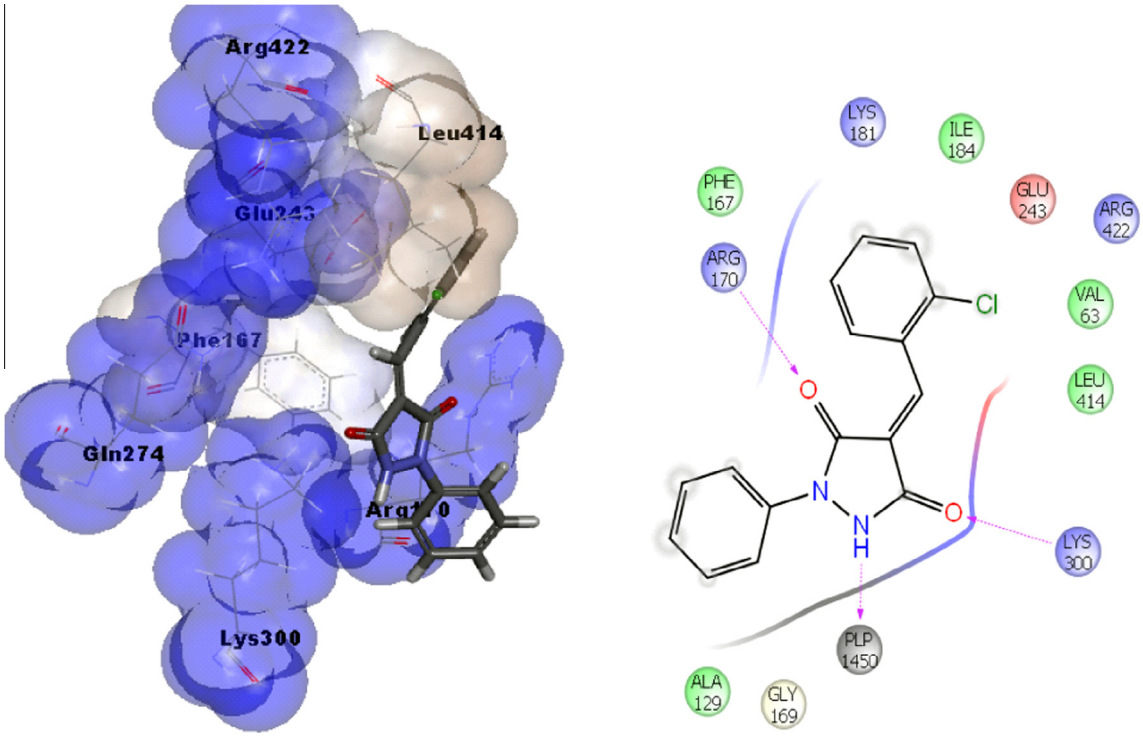

Fig. 5 – Binding pattern and protein ligand contacts of MTB LAT with the most active compound 3i.

idues (HIE44, Ser196 and HIE47), suggesting a strong inhibitor against PanC.

AlaDH catalyze NAD(H)-dependent the oxidative deamination of L-alanine to pyruvate and ammonia (catabolic reaction) or, in the reverse direction, the reductive amination of pyruvate to L-alanine (biosynthetic reaction). A recent analysis involving microarray and other data had identified this enzyme among the top three drug targets, especially against persistence [10]. Enzymatic activity was measured by the rate of production of NADH that accompanies the conversion of alanine to pyruvate by oxidative deamination [11]. The IC_{50} of the screened compounds are reported in Table 1; ten compounds inhibited MTB AlaDH with IC_{50} of $\leqslant$50 μM. Four compounds (**3k**, **3n**, **4d**, and **4n**) inhibited with IC_{50} of <15 μM, and 4-(furan-2-ylmethylene)-1-phenylpyrazolidine-3,5-dione (**3n**) was found to be a more potent compound with IC_{50} of 8.14 ± 0.09 μM. The reported crystal structure of MTB AlaDH (PDB code: 2VHW) consists of six chains, ABCDEF, respectively. The subunit of MTB AlaDH is built up of two distinct domains: NAD^+ binding domain and the substrate-binding domain. As there are no inhibitors reported for MTB AlaDH, co-factor NAD^+ bound with the protein along with substrate pyruvate is used for docking studies in this report. The reference ligand NAD^+ was re-docked with the active site residues of the MTB AlaDH protein to validate the active site cavity. The compound exhibited the highest Glide score of −11.42 kcal/mol and it docked near the vicinity of amino acids Asp270, Val298, Thr178, Ser220, Lys203, Asp198, Met301, Ile267, Ser134, Leu240 and Ala179. Here, the binding analysis of the most active compound 4-(furan-2-ylmethylene)-1-phenylpyrazolidine-3,5-dione (**3n**) in the series is reported. The most active compound **3n**, IC_{50} 8.14 ± 0.09 μM is showing a docking score of −5.79 only which showed the hydrogen bonding interaction with important amino acids such as Ala179, and Ala238, the compound that also makes the hydrophobic interaction with Leu130, Pro240, Leu240, Ala126, Ala131, Ala176, Val239 and ILE199 (Fig. 4). The active compound showing less hydrogen bonding as compared with the reference ligand NAD+; this is because the compound **3n** is small as compared with NAD+, and it occupies the smaller active site cavity. Despite its small cavity, the compound makes two hydrogen bonding interactions with important amino acid residues such as Ala179 and Ala238; also in addition, it fit well in the active site cavity. With this analysis, it was observed that the active compound **3n** showed less hydrogen bonding interaction as compared with hydrophobic interaction, which may indicate that hydrophobic interaction plays an important role. The binding pattern of compound **3n** is depicted in Fig. 4.

Another enzyme important for long-term persistence is MTB LAT. It is implicated in mycobacterial stress response and is up-regulated approximately 40-fold in nutrient-starved models designed to mimic the persistent/latent state of TB [12]. LAT also plays an important role in adaptation to long-term persistence in MTB; it catalyses an overall reaction involving the transfer of the epsilon-amino group of L-lysine to α-ketoglutarate to yield L-glutamate and alpha-aminoadipate-Δ-semialdehyde and then to piperidine 6-carboxylate. LAT activity was determined by the detection of reaction product piperidine 6-carboxylate and it was detected by measuring the color intensity of its adduct with o-amino benzaldehyde spectroscopically at 465 nm [13]. The IC_{50} of the screened compounds were reported in Table 1; 13 compounds inhibited MTB LAT with IC_{50} of $\leqslant$50 μM. Four compounds (**3i**,

4d, **4i** and **4j**) inhibited with IC_{50} of <20 μM, and 4-(2-chlorobenzylidene)-1-phenylpyrazolidine-3,5-dione (**3i**) were found to be more potent compounds with IC_{50} of 11.45 ± 0.16 μM. The reported crystal structure of MTB LAT (PDB ID: 2CJH) consists of one chain. In that protein substrate, α-ketoglutarate is bound with PMP and is crystallized. As there are no significant inhibitors reported which are co-crystallized with MTB LAT, substrate α-ketoglutarate is bound with PMP and is used for the docking studies in this report. First, the substrate α -ketoglutarate is re-docked to the active site cavity and showed a docking score of −5.28 and made two hydrogen bonding interactions with Arg170, and one with Arg422, Lys300 and Gln274 amino acid residues. This study reports the binding analysis of the most active compound 4-(2-chlorobenzylidine)-1-phenylpyrazolidine-3,5-dione (**3i**) in the series. The most active compound **3i** showed a good docking score of −5.40, which is higher than the α-ketoglutarate. The binding pattern of the compound **3i** is depicted in Fig. 5, and it clearly indicated that the oxygen atom of the pyrazolidine ring makes a hydrogen bonding interaction with Lys300; another oxygen atom of the pyrazolidine ring also makes a hydrogen bonding interaction with Arg170, while the 2-chlorobenzylidine is surrounded by some hydrophobic amino acid residues such as Val63, Leu414, and Ile184. The NH atom of the pyrazolidine ring also makes an interaction with PLP (Fig. 5). Based on this analysis, it was observed that in compound **3i** 'pyrazolidine ring and 2-chlorobenzylidine' moiety is important for activity. The compound **3i** also fits well in the active site cavity, which is surrounded by a few hydrophobic amino acids, such as Phe167, Leu414, and Ile184. Compound **3i** is also surrounded by these hydrophobic amino acid residues.

Conclusion

In this study, the SAR of various inhibitors of MTB was designed, synthesized and studied based on the reported lead compound **CD59**. To explore the possible mechanism of action of those active molecules, three MTB enzymes were screened against them. Some of the compounds were active against latent/persistent MTB targets; further screening of these molecules required *in vitro* dormant MTB models.

Conflict of interest

No conflict of interest is perceived and none declared.

Acknowledgements

G.S. is thankful to CSIR-India for providing fellowship. D.S. acknowledges University Grants Commission, New Delhi, India for UGC Research Award.

REFERENCES

[1] In World Health Organization Global Tuberculosis Control, 2012. Available at <http://www.who.int/tb/publications/global_report/en/> (accessed 18th January 2014).
[2] In Multidrug and Extensively Drug-Resistant TB (M/XDR-TB): Global Report on Surveillance and Response, 2010. Available at <http://www.who.int/tb/publications/2010/978924599191/en/index.html> (accessed 6th August 2013).
[3] D.J. Payne, M.N. Gwynn, D.J. Holmes, D.L. Pompliano, Drugs for bad bugs: confronting the challenges of antibacterial discovery, Nat. Rev. Drug. Disc. 6 (2007) 29–40.
[4] C. Vilcheze, A.D. Baughn, J. Tufariello, L.W. Leung, M. Kuo, C.F. Basler, et al, Novel inhibitors of InhA efficiently kill Mycobacterium tuberculosis under aerobic and anaerobic conditions, Antimicrob. Agents Chemother. 55 (2011) 3889–3898.
[5] S.G. Franzblau, R.S. Witzig, J.C. McLaughlin, P. Torres, G. Madico, A. Hernandez, et al, Rapid, low-technology MIC determination with clinical Mycobacterium tuberculosis isolates by using the microplate Alamar Blue assay, J. Clin. Microbiol. 36 (1998) 362–366.
[6] R. Zheng, J.S. Blanchard, Steady-state and pre-steady-state kinetic analysis of Mycobacterium tuberculosis pantothenate synthetase, Biochemistry 40 (2001) 12904–12912.
[7] V.K. Sambandamurthy, X. Wang, B. Chen, R.G. Russell, S. Derrick, F.M. Collins, S.L. Morris, et al, A pantothenate auxotroph of *Mycobacterium tuberculosis* is highly attenuated and protects mice against tuberculosis, Nat. Med. 8 (2002) 1171–1174.
[8] V.K. Sambandamurthy, S.C. Derrick, K.V. Jalapathy, B. Chen, R.G. Russell, S.L. Morris, et al, Long-term protection against tuberculosis following vaccination with a severely attenuated double lysine and pantothenate auxotroph of *Mycobacterium tuberculosis*, Infect. Immun. 73 (2005) 1196–1203.
[9] A.W. Hung, H.L. Silvestre, S. Wen, A. Ciulli, T.L. Blundell, C. Abell, et al, Application of fragment growing and fragment linking to the discovery of inhibitors of *Mycobacterium tuberculosis* pantothenate synthetase, Angew. Chem. Int. Ed. 48 (2009) 8452–8456.
[10] S. Hasan, S. Daugelat, P.S. Rao, M. Schreiber, Prioritizing genomic drug targets in pathogens: application to *Mycobacterium tuberculosis*, PLoS Comput. Biol. 2 (2006) 61.
[11] S.M. Tripathi, R. Ramachandran, Overexpression, purification, crystallization and preliminary X-ray analysis of Rv2780 from *Mycobacterium tuberculosis* H37Rv, Acta Crystallogr., Sect. F: Struct. Biol. Cryst. Commun. 64 (2008) 367–370.
[12] J.C. Betts, P.T. Lukey, L.C. Robb, R.A. McAdam, K. Duncan, Evaluation of a nutrient starvation model of *Mycobacterium tuberculosis* persistence by gene and protein expression profiling, Mol. Microbiol. 43 (2002) 717–731.
[13] S.M. Tripathi, R. Ramachandran, Overexpression, purification and crystallization of lysine epsilon-aminotransferase (Rv3290c) from *Mycobacterium tuberculosis* H37Rv, Acta Crystallogr., Sect. F: Struct. Biol. Cryst. Commun. 62 (2006) 572–575.